01 Aug 2023

Machine Learning-Based Seismic Damage Assessment Of Residential Buildings Considering Multiple Earthquake And Structure Uncertainties

Xinzhe Yuan

Liujun Li
Missouri University of Science and Technology, llpwc@mst.edu

Haibin Zhang

Yanping Zhu

et. al. For a complete list of authors, see https://scholarsmine.mst.edu/civarc_enveng_facwork/2517

Recommended Citation

X. Yuan et al., "Machine Learning-Based Seismic Damage Assessment Of Residential Buildings Considering Multiple Earthquake And Structure Uncertainties," *Natural Hazards Review*, vol. 24, no. 3, article no. 04023024, American Society of Civil Engineers, Aug 2023.
The definitive version is available at https://doi.org/10.1061/NHREFO.NHENG-1681

ASCE

Machine Learning-Based Seismic Damage Assessment of Residential Buildings Considering Multiple Earthquake and Structure Uncertainties

Xinzhe Yuan, Ph.D.[1]; Liujun Li, Ph.D.[2]; Haibin Zhang, Ph.D.[3]; Yanping Zhu, Ph.D.[4]; Genda Chen, Ph.D., P.E., F.ASCE[5]; and Cihan Dagli, Ph.D.[6]

Abstract: Wood-frame structures are used in almost 90% of residential buildings in the United States. It is thus imperative to rapidly and accurately assess the damage of wood-frame structures in the wake of an earthquake event. This study aims to develop a machine-learning-based seismic classifier for a portfolio of 6,113 wood-frame structures near the New Madrid Seismic Zone (NMSZ) in which synthesized ground motions are adopted to characterize potential earthquakes. This seismic classifier, based on a multilayer perceptron (MLP), is compared with existing fragility curves developed for the same wood-frame buildings near the NMSZ. This comparative study indicates that the MLP seismic classifier and fragility curves perform equally well when predicting minor damage. However, the MLP classifier is more accurate than the fragility curves in prediction of moderate and severe damage. Compared with the existing fragility curves with earthquake intensity measures as inputs, machine-learning-based seismic classifiers can incorporate multiple parameters of earthquakes and structures as input features, thus providing a promising tool for accurate seismic damage assessment in a portfolio scale. Once trained, the MLP classifier can predict damage classes of the 6,113 structures within 0.07 s on a general-purpose computer. **DOI: 10.1061/NHREFO.NHENG-1681.**

Introduction

Approximately 90% of the US residential buildings are constructed with lightweight wood-frame structures. These residential buildings are generally lightweight, flexible, and redundant in resistance, which are desirable properties in buildings when subjected to large earthquakes. However, significant vulnerabilities in wood-frame construction have been observed during historical earthquakes in the US. For example, the property loss of wood-frame buildings during the 1994 Northridge Earthquake in California was estimated to be over $20 billion, which significantly exceeded the loss associated with any other type of construction (Kircher et al. 1997). More critically, 24 of the 25 fatalities caused during the earthquake were associated with wood-frame buildings (Ellingwood et al. 2008). One reason for these high consequences was the nonengineered or partially engineered design of wood structures in seismic regions (Ellingwood et al. 2008; Filiatrault et al. 2010). To better understand and improve the seismic performance of wood-frame buildings, many numerical and experimental studies have been conducted to investigate the dynamic characteristics such as fundamental periods and damping (Camelo 2003; Hafeez et al. 2018), seismic performance (Filiatrault et al. 2010; van de Lindt et al. 2010; Lucksiri et al. 2012a; Pei et al. 2013), and post-earthquake damage and loss assessment of the wood-frame buildings (Chase et al. 2019; Ellingwood et al. 2004; van de Lindt 2005; Lucksiri et al. 2012b). For rapid post-event damage assessment in a high seismicity region, fragility curves are usually generated for a class of buildings with similar structural properties. For example, a set of fragility curves for one-story wood-frame residential buildings in Memphis, Tennessee, was generated by Ellingwood et al. (2008). These fragility curves can be used to rapidly estimate the probabilities of different damage states of wood-frame structures through a single intensity measure (IM), such as the spectral acceleration (Sa) at the fundamental period of a structure.

Although computationally efficient (Zhao et al. 2021), these fragility curves based on a single IM may not sufficiently capture the primary uncertainty of earthquakes in fragility estimation. Therefore, alternative fragility models based on multiple IMs were developed for the fragility estimation (Baker and Cornell 2005; Du et al. 2020). Moreover, the fragility curves for a class of structures do not use structural parameters as inputs, like the years of constructions, plan configurations, and structural weights. These uncertainties can have a significant impact on the seismic performance of wood structures (Kim et al. 2006; Lucksiri et al. 2012a, b; Scotta et al. 2018). According to Kim et al. (2006), the sheathing-to-framing connection of shear walls, which are primary members to resist earthquake loadings, suffered a more than 50% loss of

[1]Formerly, Research Associate, Dept. of Civil, Architectural and Environmental Engineering, Missouri Univ. of Science and Technology, Rolla, MO 65401. ORCID: https://orcid.org/0000-0003-4567-5362. Email: xyvm4@mst.edu

[2]Assistant Professor, Dept. of Soil and Water System, Univ. of Idaho, Moscow, ID 83844. Email: liujunl@uidaho.edu

[3]Research Consultant, Dept. of Civil, Architectural and Environmental Engineering, Missouri Univ. of Science and Technology, Rolla, MO 65401. Email: zhanghaib@mst.edu

[4]Postdoctoral Fellow, Dept. of Civil, Architectural and Environmental Engineering, Missouri Univ. of Science and Technology, Rolla, MO 65401. Email: yz6d7@mst.edu

[5]Professor, Dept. of Civil, Architectural and Environmental Engineering, Missouri Univ. of Science and Technology, Rolla, MO 65401 (corresponding author). ORCID: https://orcid.org/0000-0002-0658-4356. Email: gchen@mst.edu

[6]Professor, Dept. of Engineering Management and Systems Engineering, Missouri Univ. of Science and Technology, Rolla, MO 65401. Email: dagli@mst.edu

Note. This manuscript was submitted on June 12, 2022; approved on February 27, 2023; published online on May 5, 2023. Discussion period open until October 5, 2023; separate discussions must be submitted for individual papers. This paper is part of the ***Natural Hazards Review***, © ASCE, ISSN 1527-6988.

maximum loading capacity, stiffness, ductility, and energy dissipation due to 30 weeks of fungal attacks. Besides, failure probabilities of the shear walls with the 30-week deterioration were approximately 60% higher than those of the shear walls without deterioration. Although regular maintenance and repair can delay the deterioration of wood-frame structures, the decay of wood components is inevitable. Therefore, structural uncertainties such as the built year of wood-frame construction should be considered in the post-earthquake damage assessment in addition to the primary uncertainty of earthquakes, which is difficult to take into account in the approach of fragility curves.

In recent years, machine learning and deep learning technologies have been increasingly applied to post-earthquake damage assessment of reinforced concrete (r/c) structures and infrastructure (Du and Padgett 2020; Du et al. 2020; Lagaros and Fragiadakis 2007; Xu et al. 2020; Lu et al. 2021; Yang et al. 2023; Yuan et al. 2021). Among these applications, the multiplayer perceptron (MLP), i.e., a class of feedforward artificial neural networks (ANNs), is widely used for continuous seismic demand regression (de Lautour and Omenzetter 2009; Mangalathu et al. 2018; Wang et al. 2018) and seismic damage multiclassification (Kostinakis and Morfidis 2020; Morfidis and Kostinakis 2018, 2019). The input layer of the MLP consists of many input neurons. Thus, multiple parameters representing the uncertainties of earthquakes and structures can be inputted to the MLP. By propagating these input parameters to the output layer, the neurons in the output layer provide the estimation of seismic responses or damage states of a structure under a specific earthquake excitation. For instance, de Lautour and Omenzetter (2009) used six IMs of ground motions and 13 parameters of structures as inputs of the MLP model to estimate the continuous Park-Ang damage values of r/c frame buildings. The study of Morfidis and Kostinakis (2018) used 14 IMs and four structural parameters as inputs of the MLP model to classify the damage states of 30 r/c buildings. Yuan et al. (2022) developed an MLP model with multiple IMs as inputs for the simultaneous fragility estimation and damage classification of a four-story benchmark r/c frame building. These previous studies indicate that the machine learning-based seismic damage assessment approaches can incorporate more input parameters to better propagate the uncertainties of ground motions and structures than the traditional statistical fragility curves. However, despite the extensive applications to r/c structures and infrastructure, this machine-learning-based approach is rarely applied to wood-frame structures. Yi and Burton (2020) and Yi (2020) used the extreme gradient boosting (XGBoost) model for continuous seismic demand estimation of soft-story wood buildings in California. Studies of machine-learning-based seismic classifiers for the damage classification of wood-frame constructions and comparison with traditional fragility curves, to the best knowledge of the authors, have not been conducted.

This study develops multivariate MLP seismic classifiers for single-family one-story wood-frame constructions near the New Madrid Seismic Zone (NMSZ). This portfolio of wood-frame structures is approximately 60 km (40 mi) to the southwest end of the (NMSZ), where a sequence of three main shocks over Magnitude 8 happened during 1811–1812. Researchers have developed traditional single-IM fragility curves for the wood-frame residential buildings near NMSZ (Ellingwood et al. 2008). The newly proposed multivariate MLP seismic classifiers in this study use six IMs of ground motions and two structural parameters of the wood construction to span the input feature space. The six IMs include the acceleration response spectrum (Sa) at the fundamental period (T_f) and five readily available IMs from ShakeMap (Wald et al. 2006). The ShakeMap provides the peak ground acceleration (PGA), peak ground velocity (PGV), and Sa at 0.3, 1.0, 3.0 s. The effectiveness of the five readily available IMs has been validated in an MLP seismic classifier of a r/c frame structure (Yuan et al. 2022). The two input structural parameters are the built years and gross areas that have an impact on the dynamic structural performance. Other structural parameters such as plan irregularity, number of stories, and window/door openings are also critical to the performance of wood-frame residential buildings according to Lucksiri et al. (2012a, b). However, these parameters are not included as inputs in this study due to their unavailability. As the number of strong historical ground motions in the Central and Eastern United States (CEUS) is limited, this study adopts a set of 120 synthesized ground motion records generated for three cities (Memphis, Tennessee; St. Louis, Missouri; and Carbondale, Illinois) near NMSZ (Wen et al. 2001) to conduct the nonlinear time history analyses (NLTHA) for training. Another set of 12 ground motion records (Atkinson and Beresnev 2002) generated for two cities (Memphis and St. Louis) are collected for the test and comparison of trained MLP seismic classifiers and the fragility curves generated by Ellingwood et al. (2008).

This paper is organized as follows. The "Multilayer Perceptron" section introduces the MLP seismic classifier models. The "Wood-Frame Portfolio and Earthquake Ground Motions" section provides the details of selected ground motions and wood-frame residential buildings. The "MLP Seismic Classifier Training, Testing, and Comparison" section deals with the MLP training, testing, and comparison with traditional fragility curves. The "Results and Discussion" section discusses the obtained results. The "Conclusions" section concludes the findings and presents the future research directions to improve the MLP seismic classifiers.

Multilayer Perceptron

The MLP is a class of feedforward ANNs. Each ANN consists of an input layer, hidden layers, and an output layer. The neurons on each layer simulate the neurons in human brains to pass information. The input layer includes the selected features (IMs and structural parameters in this study), and its neuron number is determined by the number of input features. The output layer includes the damage states of structures in this study, and its neuron number is determined by the number of desired damage states. The number of hidden layers and neurons in each hidden layer, however, can be flexible to result in desirable outputs. There is no unique definition for the optimal size of hidden neurons for the MLP with one or two hidden layers (Morfidis and Kostinakis 2018). Since the optimal size of the hidden layers and hidden neurons is not in the scope of this study, an MLP configuration with two hidden layers and 20 neurons in each hidden layer, as shown in Fig. 1, is considered in this study based on the practical range recommended by Morfidis and Kostinakis (2018).

As shown in Fig. 1, the neurons in two adjacent MLP layers are fully connected to imitate the synaptic connection of human brain neurons. Each connection is assigned with a weight factor. The weight factors between the two adjacent layers are collected to form a weight matrix. The output signal from the previous layer, in the form of a vector, is multiplied by the weight matrix to determine an input signal u to the current layer. Then, the input signal u goes through the activation function before it is passed on as an output signal to the next layer. The activation function σ_1 of the hidden layers is set to a hyperbolic tangent function, as recommended by Morfidis and Kostinakis (2018). The activation function σ_2 of the output layer is the softmax function, which is commonly used in MLP multiclassification tasks (Ren et al. 2017). The softmax function outputs a probability vector p for the final classification of damage states in wood-frame buildings. Each element of the vector p corresponds to the probability of one damage class.

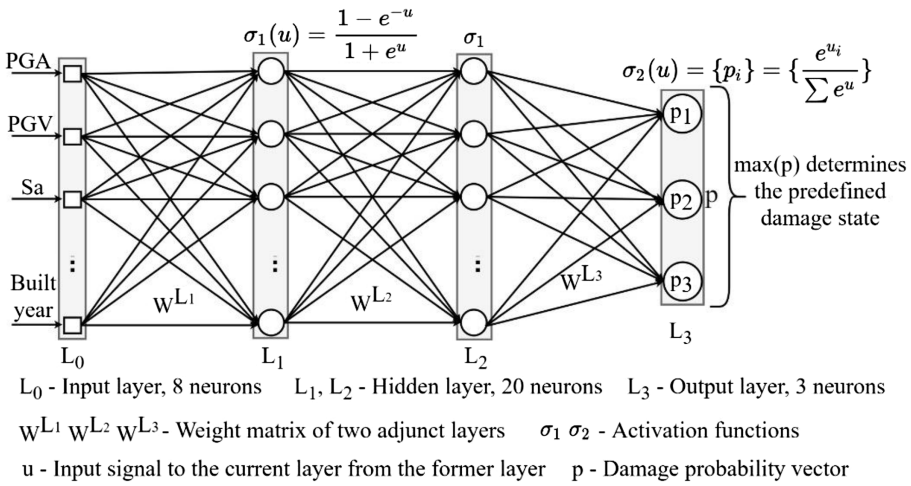

Fig. 1. Configuration of the proposed MLP seismic classifier.

The input vector, which represents a structure in the selected wood-frame portfolio when excited by an earthquake ground motion, will be predicted to the damage class corresponding to the largest probability. Three performance levels of the wood-frame construction are included in the FEMA 273/356 Provisions (FEMA 1997): immediate occupancy (IO); life safety (LS); and collapse prevention (CP). Since the fragilities for the CP performance level are small within the selected *Sa* range as demonstrated by Ellingwood et al. (2008), only IO and LS performance levels are considered in this study. Accordingly, three damage classes divided by the two performance levels of IO and LS are denoted as minor, moderate, and severe.

Table 1 summarizes the input and output parameters used in the MLP configuration, as shown in Fig. 1. Once its configuration is determined, the MLP seismic classifier needs to learn from a labeled training data set to achieve a desirable prediction accuracy on future unseen earthquakes, following the supervised learning method (Caruana and Niculescu-Mizil 2006). The data for the training of the MLP seismic classifier are usually obtained from NLTHA (Kostinakis and Morfidis 2020; Morfidis and Kostinakis 2018, 2019). The NLTHA of a structure under an earthquake excitation (i.e., ground motion) generates a seismic damage class of the structure, forming one training sample comprised of an input vector (six IMs and two structural parameters) and its corresponding damage class. With many different training samples iteratively fed into the MLP seismic classifier, its synaptic weight matrices are tuned and updated to achieve satisfactory performance on the training data set and a separate testing data set. The testing data set does not get involved in the MLP training process or the weight tuning.

Table 1. Input and output parameters in the MLP seismic classifier

Layer	Parameters	Sources
Input	Six IM parameters, the PGA, PGV, $Sa_{t=0.3s}$, $Sa_{t=1.0s}$, $Sa_{t=3.0s}$, $Sa_{t=Tf}$, and two structural parameters, the built years and the gross areas.	Six IM parameters are selected considering their ready availability and effectiveness, according to studies by Wald et al. (2006), Ellingwood et al. (2008), and Yuan et al. (2022).
Output	Three damage states: minor; moderate; and severe.	Three damage states are determined according to studies of FEMA (1997), and Ellingwood et al. (2008).

Instead, it is mainly used to ensure the trained MLP performs well on an unseen future earthquake other than the experienced training earthquakes. Once well trained, the MLP seismic classifier can be used to conduct a near real-time damage assessment during future earthquakes.

Wood-Frame Portfolio and Earthquake Ground Motions

Wood-Frame Portfolio of One-Story Residential Buildings

Despite the continuing evolution of housing characteristics in the US, residential construction practices have been rarely changed in the past 40 years. Wood-frame residential buildings generally fall in the range of one to three stories in height and are dominated by one- or two-story structures. Similar to Ellingwood et al. (2008) and Pang et al. (2009), one-story wood-frame residential buildings near the NMSZ are the focus in this study. A typical wood-frame portfolio in Joplin, Missouri, is adopted for the portfolio case study, as wood-frame residential buildings are believed to have similar construction practices from the west US (WUS) to the CEUS, with similar numbers of stories, footprint, or even dynamic characteristics, e.g., distribution of mass, building height, and natural period (Ellingwood et al. 2008). This portfolio, similar to the building types in the Joplin testbed by Attary et al. (2018) and Memari et al. (2018), can be obtained in the interdependent networked community resilience modeling environment (IN-CORE) by Gardoni et al. (2018). This website provides 10,465 one-story residential wood-frame buildings with regular plan configurations, years of construction and gross areas. Since the gross areas of the 10,465 buildings vary substantially from 0.09 m^2 to 2,187 m^2, only 6,113 buildings with gross areas of 93 m^2 to 232 m^2 are selected from the 10,465 buildings for this portfolio study, which house a family of three to six members. The year of construction in the filtered portfolio of buildings varies from 1840 to 2010. The one-story residential wood-frame portfolio is depicted in Fig. 2.

For the portfolio-scale seismic damage assessment, the simplified and idealized structural models are generally preferred in the NLTHA of a large number of buildings for the sake of computational efficiency. Surrogate single-degree-of-freedom (SDOF) models were proposed to simulate multistory buildings in Karimzadeh et al. (2018) and Vaseghiamiri et al. (2020). The one-story wood-frame

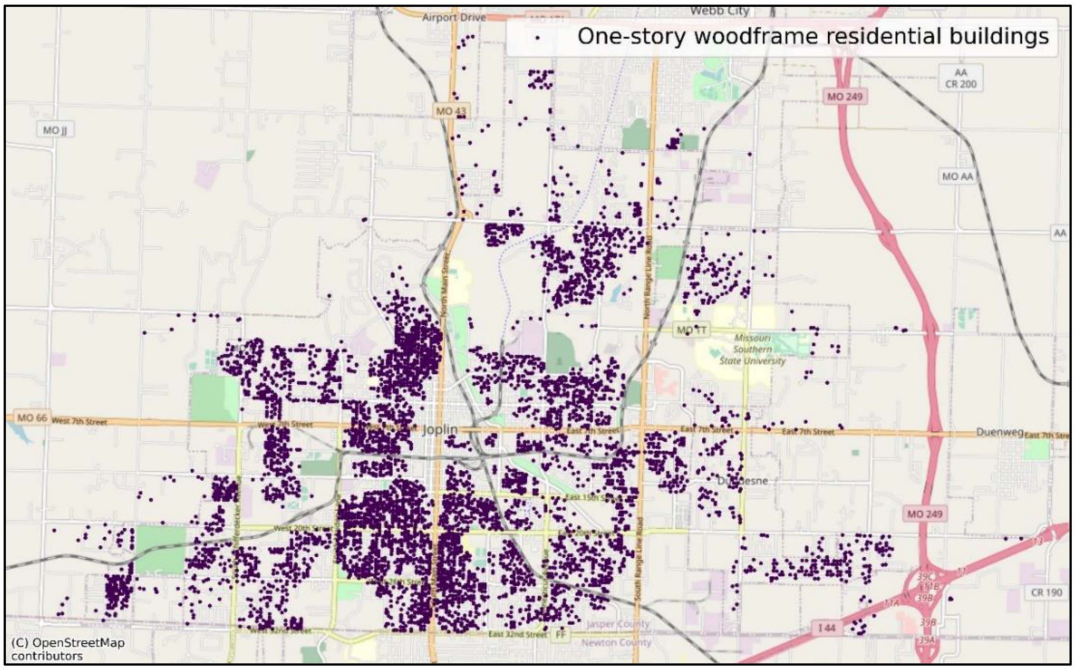

Fig. 2. One-story wood-frame building portfolio in Joplin, Missouri. (Base Map © OpenStreetMap contributors.)

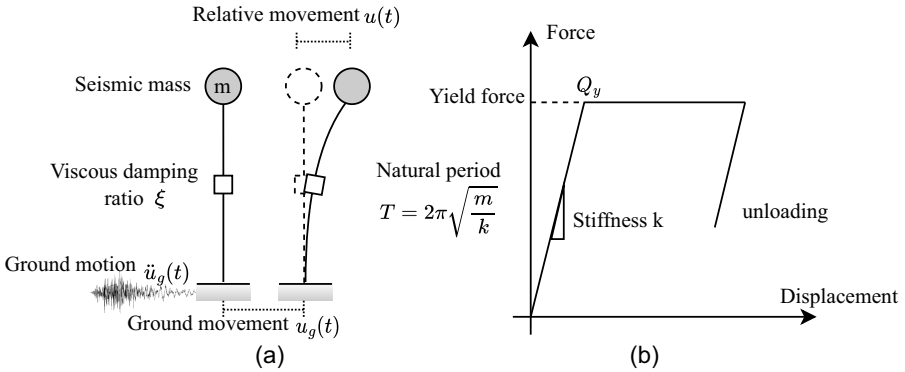

Fig. 3. One-story wood-frame structures: (a) SDOF model; and (b) force-displacement relationship.

structures in the portfolio of this study are simulated by a general SDOF model with a uniaxial elastic-perfectly plastic force-displacement relationship, following the protocol of the parameterized fragility method (PFM) in Jeong and Elnashai (2007). Fig. 3 shows the SDOF model and its force–displacement relationship.

The dynamic characteristics of the SDOF model in Fig. 3 are mainly determined by its structural mass m, elastic stiffness k, damping ratio ξ, and yield force Q_y. The natural period of the model at low vibration can be computed from m and k, as shown in Fig. 3. Corresponding to the selected range of gross area in the studied wood-frame portfolio, the seismic weight ranges from 1.1 kN/m^2 to 2.0 kN/m^2, as reported in Pang et al. (2009) and Filiatrault et al. (2010). The upper bound of the seismic weight, 2 kN/m^2, is used in this study. On the other hand, the built year of wood structures varies from 1840 to 2010. As shown in Kim et al. (2006) and Scotta et al. (2018), fungal attack and moisture could result in the degradation of wood structures in stiffness, energy dissipation, lateral resistance, and ductility by up to 50%. Therefore, a linear degradation relationship of structural properties is assumed from 2010 to 1840. That is, the mean elastic stiffness k, mean damping ratio ξ, and mean yield force Q_y of a one-story wood-frame residential building built in 1840 are set to 50% of the corresponding properties of buildings when built in 2010. The mean values of the elastic stiffness k, damping ratio ξ, and the yield force Qy of a baseline 2010 structure are assumed to be 100 kN/cm, 10%, and 60 kN based on previous experimental and computational studies of wood-frame residential buildings (Camelo 2003; Filiatrault et al. 2010; Hafeez et al. 2018; Kasal et al. 2004; Pei et al. 2013; Chen et al. 2010). Thus, the mean values of the structures built between 1840 and 2010 can be estimated by the linear degradation relationship. To consider their uncertainties, the elastic stiffness k, damping ratio ξ, and the yield force Qy are assumed to follow normal distributions with a standard deviation of 2.5 kN/cm, 1%, and 2.5 kN, respectively, regardless of the year when the residential buildings are constructed. Similarly, the height of the one-story structures is assumed to follow a uniform distribution between 2.5 and 2.7 m. The structural properties of the

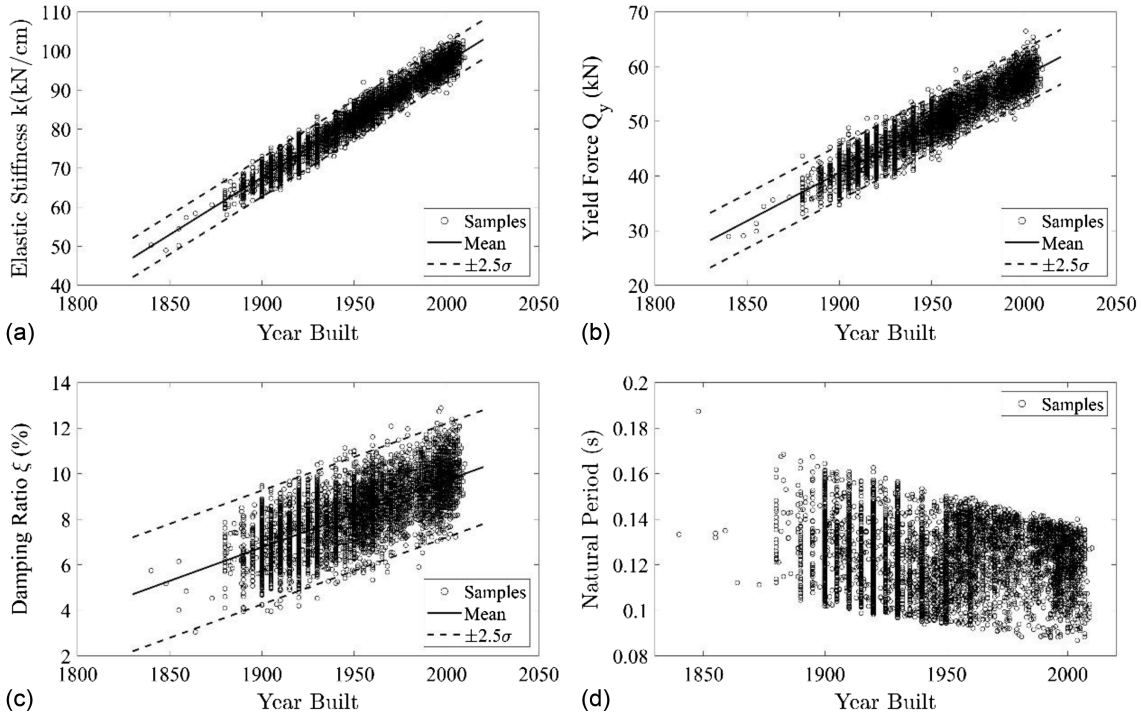

Fig. 4. Structural properties of the wood-frame portfolio: (a) elastic stiffness; (b) yield force; (c) damping ratio; and (d) computed natural period.

6,113 one-story wood-frame residential buildings are shown in Fig. 4. Figs. 4(a–c) show the randomly generated elastic stiffness k, damping ratio ξ, and the yield force Qy of the 6,113 wood-frame structures. Fig. 4(d) presents the computed natural periods of these structures. The computed natural periods range from 0.087 to 0.187 s, which are reasonably bounded by 0.06 and 0.25 s as given by Soltis and Falk (1992) and Camelo (2003). On the other hand, considering the ductility degradation of wood structures, the IO performance drift levels are 0.5%, 0.75%, and 1%, and the LS drift levels are 1%, 1.5%, and 2% for wood-frame structures built prior to 1950, between 1950 and 2000, after 2000, respectively.

Earthquake Ground Motions in NMSZ

As mentioned in the Introduction, two sets of synthesized ground motions for the NMSZ are collected to train and test the MLP seismic classifier, as there are not enough recorded strong historical ground motions in the CEUS. Herein, 120 ground motions developed by Wen et al. (2001) as part of the Mid-America Earthquake (MAE) research program are inputted into the building portfolio for training. Among these 120 ground motions, uniform hazard ground motions representing the 2% and 10% probabilities of exceedance in 50 years, were developed, respectively. Each ensemble has 60 ground motions. On the other hand, the testing set of 12 synthesized ground motions with magnitude 7.5–8 were generated by Atkinson and Beresnev (2002) from tectonic faults in the NMSZ. The elastic acceleration spectra of these synthesized ground motions with a damping ratio of 5% are shown in Fig. 5.

The maximum *Sa* values of the training and testing sets are 2.40 and 0.97 g, respectively. According to the fragility curves developed by Ellingwood et al. (2008) and Pang et al. (2009), the LS fragility of the one-story wood-frame residential building in the NMSZ is less than 50% when *Sa* is smaller than 2.5 g. The ground motions in the training set hardly cause severe damage that exceeds the LS performance level. To obtain severe-class training examples for the MLP seismic classifier, the ground motions of the training set are scaled by 2.5 times, which is substantially lower than a scale factor of 10, above which large biases are expected in seismic structural responses (Luco and Bazzurro 2007).

The scaled ground motions are applied to wood-frame structures in the studied portfolio to determine structural behavior and damage levels. To save the computational time in NLTHA, the 6,113 structures are divided into 120 groups. Each of 119 groups includes 51 structures while the last group has 44 structures only. Each group is randomly paired with a ground motion from the training set. Thus, the NLTHA generates 6,113 training samples for the MLP classifier training. The main purpose of this division is to significantly reduce the computational time in the NLTHA while maintaining a diverse training feature space of structures and ground motions.

MLP Seismic Classifier Training, Testing, and Comparison

Training

As illustrated in Fig. 1, each NLTHA learning sample for the MLP training consists of eight features: the year of construction; the gross area of the target structure; PGA; PGV; and four *Sa* values at 0.3, 1.0, 3.0 s; and the fundamental period, respectively. Because the units and scales of the eight features are quite different, the input feature data of the 6,113 NLTHA samples are normalized to improve the classification performance (Singh and Singh 2020) by Eq. (1)

$$x_{\text{norm}} = \frac{x - x_{\min}}{x_{\max} - x_{\min}} \tag{1}$$

where $x_{\min}$ and $x_{\max}$ = the minimum and maximum of an input feature, respectively; and $x_{\text{norm}} \in [0, 1]$ is the normalized feature

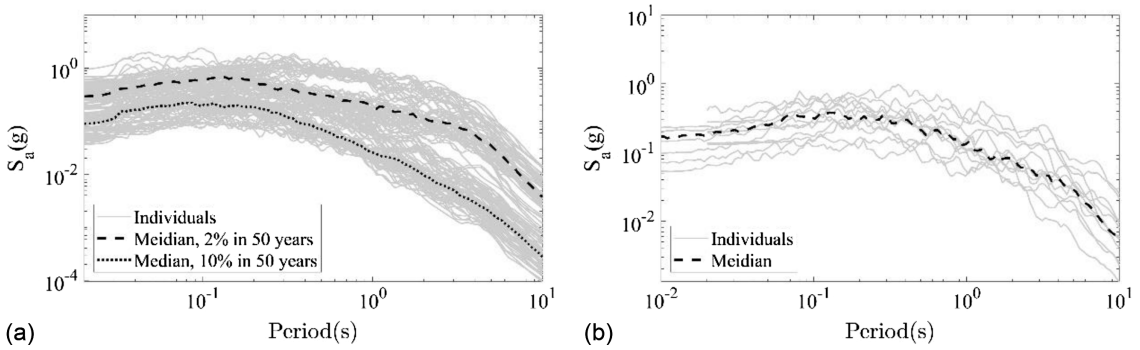

Fig. 5. Spectral accelerations (5% damping ratio) of two sets of synthesized ground motions: (a) the training set; and (b) the testing set.

of x. The damage class of each NLTHA sample is denoted by the one-hot encoding technique (Cerda et al. 2018), where the minor class is encoded as [1, 0, 0], the moderate class is encoded as [0, 1, 0], and the severe class is encoded as [0, 0, 1]. The 6,113 training samples are divided into three subsets with a ratio of 0.75: 0.15:0.15 for training, validation, and testing. The training subset is used to tune the synaptic weight matrices, as shown in Fig. 1. The validation subset is used to monitor the performance of the MLP classifier and stop the training process when the MLP classifier starts to perform poorly on the testing data (unseen future data) to avoid overfitting. An overfitted MLP classifier would perform well on the training data set (seen data) only, which is not desirable in application. The testing subset is created to test the potential bias of the trained MLP classifier with the training subset.

After the normalization of the input features, encoding of the output damage states, and the division of the NLTHA samples, the MLP seismic classifier for the one-story wood-frame portfolio is trained in the MATLAB 2020a environment. The scaled conjugate gradient backpropagation algorithm is used for weight tuning. To train the MLP classifier properly, six key training parameters are set to epochs = 1,000, learning rate lr = 0.01, training performance goal = 0, minimal performance gradient min_grad = 10^{-6}, maximal validation failure max_fail = 10, and training time = ∞. The training process is stopped when any of the epochs, goal, min_grad, or max_fail reaches its set value. These hyperparameters are critical to ensuring model performance and saving training time. For example, epochs governs the maximal training epochs, which should be large enough to ensure the training does not stop early with an underfitting model. The learning rate lr is vital in controlling the training speed and should be a small number. However, a too-small lr will result in excessive training time and thus should be avoided. The training performance goal and minimal performance gradient min_grad set up the thresholds when the loss function is minimized. Thus, goal and min_grad should be tiny nonnegative numbers. The parameter max_fail will also terminate the training when failures of the validation subset reach the setup max_fail. The training time mainly determines the maximal training time, which is set to infinite to guarantee sufficient training time. These parameters are carefully selected according to Demuth and Beale (2002) guidance for the MATLAB neural network module.

Fig. 6 shows the receiver operating characteristic (ROC) curves of the MLP prediction on the three damage classes. The ROC curve of one damage class is generated by plotting the true positive rate (TPR) against the false positive rate (FPR), which are calculated with Eqs. (2) and (3), respectively

$$\text{TPR} = \frac{\text{TP}}{\text{TP} + \text{FP}} \tag{2}$$

$$\text{FPR} = 1 - \frac{\text{TN}}{\text{TN} + \text{FP}} \tag{3}$$

where TP = the number of true positive predictions; FP = the false positive predictions; and TN = the true negative predictions by the MLP classifier for each damage class. A perfect classifier is represented by the (1, 0) point in the ROC plotting, meaning that the TPR is 100%, while the FPR is 0%. Therefore, the closer the apex of the ROC curves toward the upper-left corner, the greater discriminatory ability of the MLP classifier (Fan et al. 2006). The ROC curves in Fig. 6 are generally close to the ideal (1,0) point, indicating good discriminatory ability of the MLP classifier.

Portfolio Testing Scenarios

The 12 separate synthesized ground motions in Fig. 5(b) are used to further test the predictability of the trained MLP classifier. The maximal *Sa* of the 12 testing ground motions is 0.97 g. Based on the fragility curves developed by Ellingwood et al. (2008) and Pang et al. (2009), ground motions with *Sa* smaller than 1.0 g cause minor damage to one-story wood-frame residential buildings with a probability over 80%. The NLTHA of the 6,113 wood-frame structures confirms that the 12 ground motions all induce minor damage to the wood-frame portfolio. To generate the severe damage samples of the wood-frame portfolio during testing, the 12 ground motions are scaled with a factor of 5 to increase their earthquake intensities. According to previous research on the impact of ground motion scaling to seismic structural responses (Haselton et al. 2008; Luco and Cornell 2007), a scale factor of 5 is acceptable and will not result in a significant bias in the NLTHA results.

Two portfolio testing scenarios, Scale 1 (no scaling) and Scale 5 of the 12 ground motions, are utilized as unseen future earthquakes to test the trained MLP seismic classifier for the studied wood-frame portfolio. The prediction accuracy of a predictive model (either MLP classifier or fragility curves) is used in the portfolio testing to measure the model performance, which can be calculated from Eq. (4)

$$\text{accuracy} = \frac{\text{number of buildings classified to the right damage state}}{\text{total number of buildings}} \tag{4}$$

Fig. 7 shows the two testing scenarios of one ground motion record. Compared with the NLTHA ground-truth results, the MLP

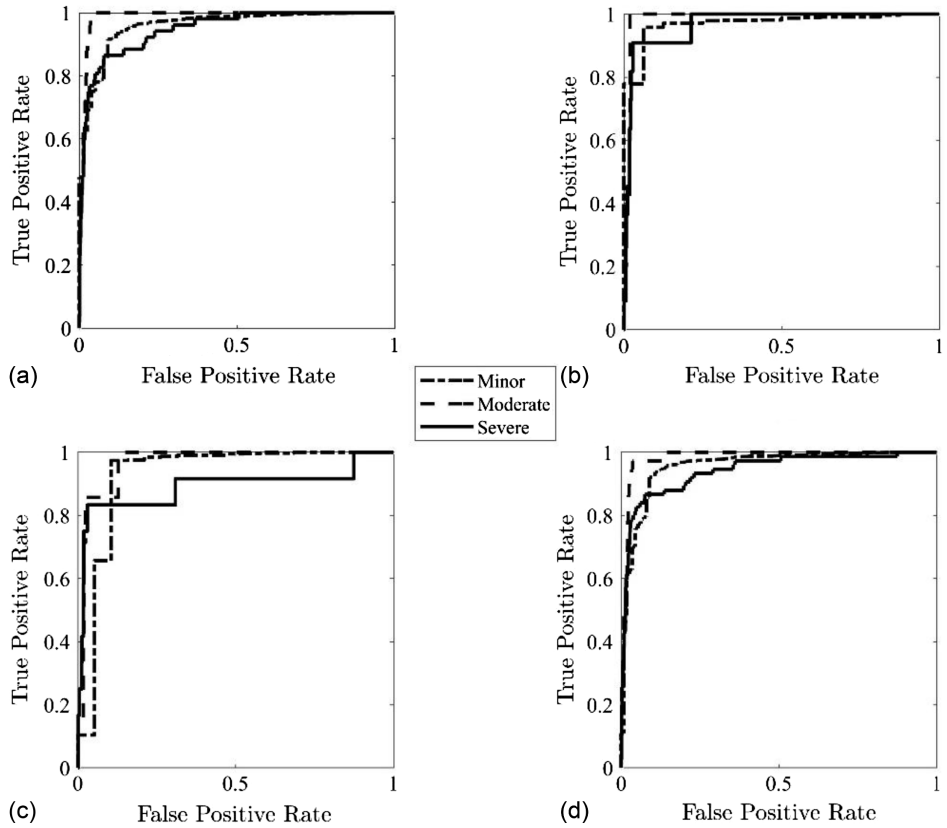

Fig. 6. Receiver operating characteristics of three damage classes in different data sets: (a) training subset; (b) validation subset; (c) testing subset; and (d) all three subsets combined.

seismic classifier achieves 100% accuracy in the Scale 1 scenario and 92% in the Scale 5 scenario. These results indicate generally good predicting capacity of the MLP seismic classifier for the wood-frame portfolio under this specific testing ground motion. Fig. 8 shows the MLP prediction accuracies of the 12 testing ground motions under Scale 1 and Scale 5 scenarios. The MLP seismic classifier achieves 100% accuracy under the Scale 1 scenario. However, under the Scale 5 scenario, when the testing ground motion becomes intensified, the MLP seismic classifier does not achieve high predicting accuracies on several scaled ground motions. The reasons for these lower-accuracy predictions will be explored in "Results and Discussion" section.

Comparison with Fragility Curves

Fig. 9 presents the fragility curves developed for one-story wood-frame residential buildings near the NMSZ (Ellingwood et al. 2008). These curves were based on a critical shear wall with the most significant lateral displacement in the static pushover analysis. The shear wall was fully fixed to the sill and foundation, corresponding to the fixed-base SDOF model in Fig. 3(a). The three damage states divided by the IO and LS fragility curves are represented by three areas denoted in Fig. 9. The probabilities of the three damage states at a certain *Sa* level can be estimated from the IO and LS fragilities. The damage state can then be determined by the largest probability, following the protocol of the MLP output activation function in Fig. 1. Figs. 10 and 11 show the comparison of prediction accuracies of the MLP seismic classifier and the fragility curves in Scale 1 and Scale 5 scenario, respectively. Fig. 10 indicates that the MLP seismic classifier and fragility curves predict well with 100% accuracy when the structure responses are elastic or with weak nonlinearity. When the testing ground motions are scaled to result in strong nonlinearity of the structural responses, the MLP seismic classifier and the fragility curves both underperform in the Scale 5 scenario, as evidenced in Fig. 11.

In the Scale 5 testing scenario, the fragility curves and MLP classifier generally achieve an average accuracy of 58.1% and 85.0%, respectively. Specifically, the MLP seismic classifier and fragility curves are 100% accurate under five individual testing ground motions. For the other seven testing ground motions, the MLP seismic classifier is 13% to 95% more accurate than the fragility curves. The underperformance of the fragility curves is likely because the existing fragility curves were developed based on the NLTHA results of one or several newly built representative structures in the studied region without considering structural differences and aging factors. However, the portfolio structure population in the studied area had large structural uncertainties, such as variant deterioration, structural strength, ductility, and damage limits. In contrast, the MLP seismic classifier incorporates more structural parameters and IMs to propagate the structural and ground motion uncertainty in the seismic damage assessment process, appropriately taking the variability of individual buildings in the wood-frame portfolio into account and thus accurately predicting damage conditions at the portfolio scale. The trained MLP classifier takes approximately 0.07 s to assess damage classes of the 6,113 structures in the wood-frame portfolio on a general-purpose computer. Therefore, the MLP seismic classifier is also feasible for near real-time, portfolio-scale seismic damage assessment at a low computational cost.

Results and Discussion

In comparison with Fig. 10, Fig. 11 indicates that the prediction accuracy of the MLP classifier and fragility curves for the Scale

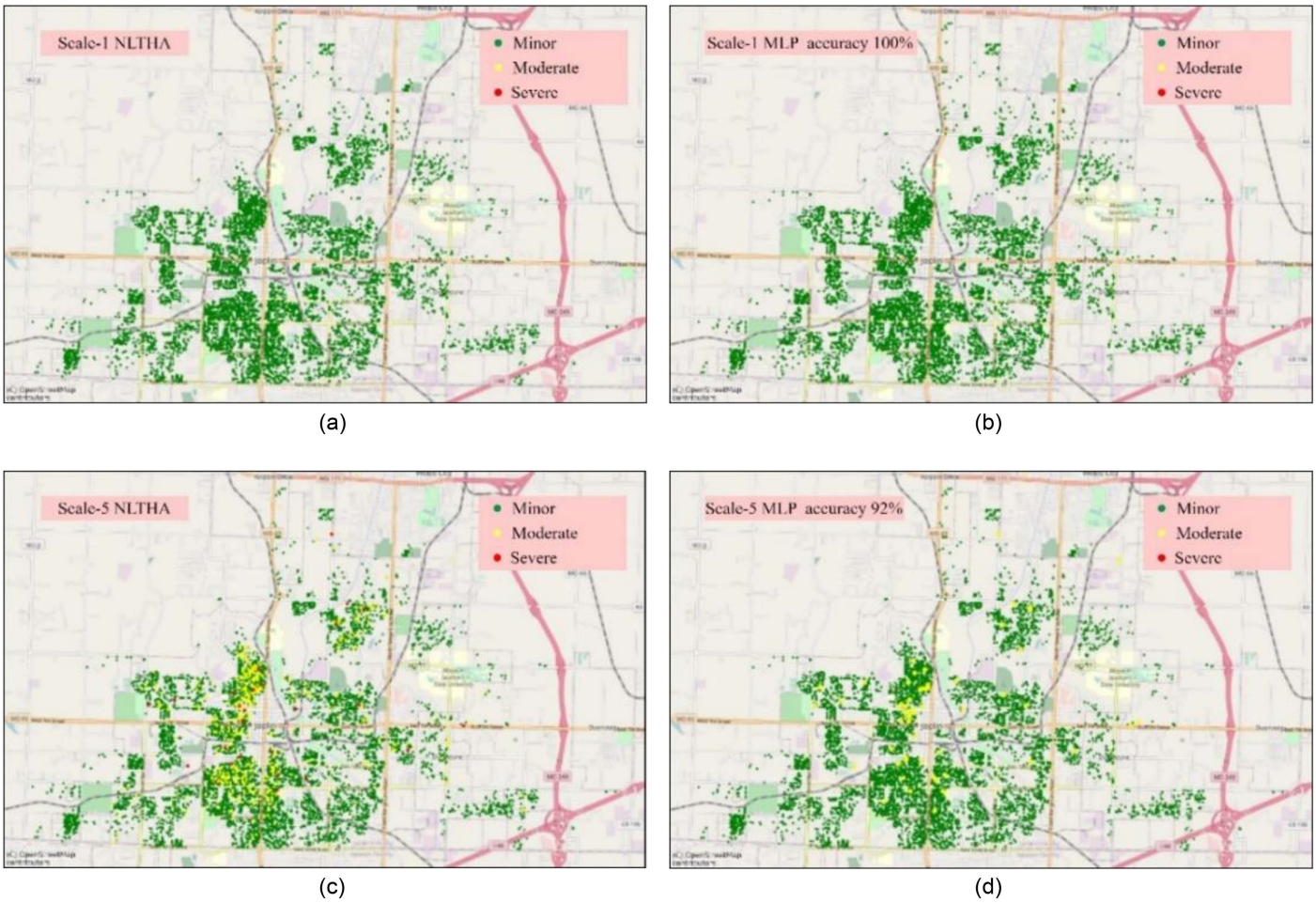

Fig. 7. NLTHA simulated versus MLP predicted damage classes at two ground motion scales: (a) Scale 1 NLTHA results; (b) Scale 1 MLP results; (c) Scale 5 NLTHA results; and (d) Scale 5 MLP results. (Base Map © OpenStreetMap contributors.)

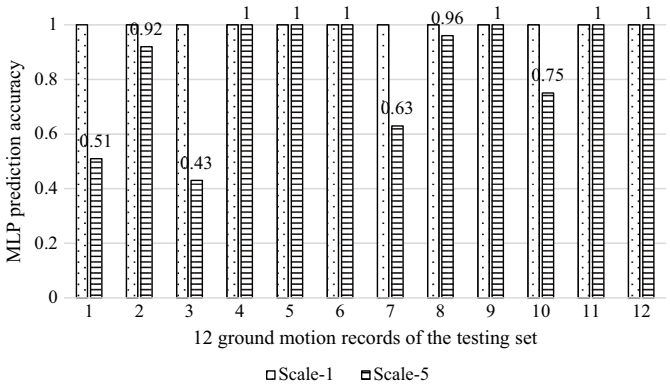

Fig. 8. MLP prediction accuracies of the 12 testing ground motions under Scale 1 and Scale 5 scenarios.

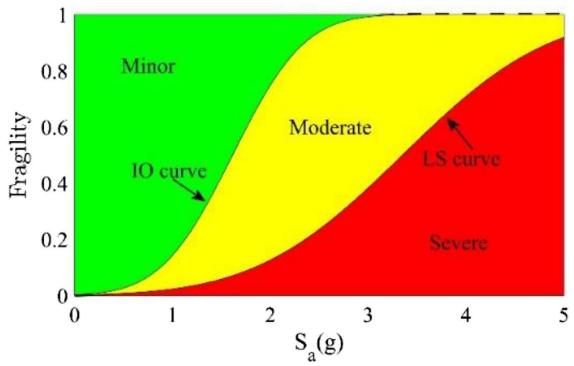

Fig. 9. Fragilities of one-story wood-frame residential buildings (fully anchored) in Memphis, Tennessee. (Data from Ellingwood et al. 2008.)

5 testing scenario is lower than that for the Scale 1 testing scenario. This is primarily because the moderate and severe damage samples in the NLTHA data are sparse for the MLP seismic classifier and traditional fragility curves, which is a common challenge for the application of machine-learning-based seismic damage assessment (Lu et al. 2021; Xu et al. 2020; Yuan et al. 2021). Among the 6,113 training samples, there are 6,001 minor samples, 37 moderate samples, and 75 severe samples. This nonuniform distribution of sample data, skewed to the minor class, makes the MLP seismic classifier more accurate when it classifies the input sample to the minor class. The fundamental reason for an insufficient number of moderate and severe samples for training lies in the sparsity of natural and synthesized strong motions in the specific site near the NMSZ. In addition, the synthesized ground motions (Atkinson and Beresnev 2002; Wen et al. 2001) collected in this study were developed based on a finite-fault model that cannot capture the

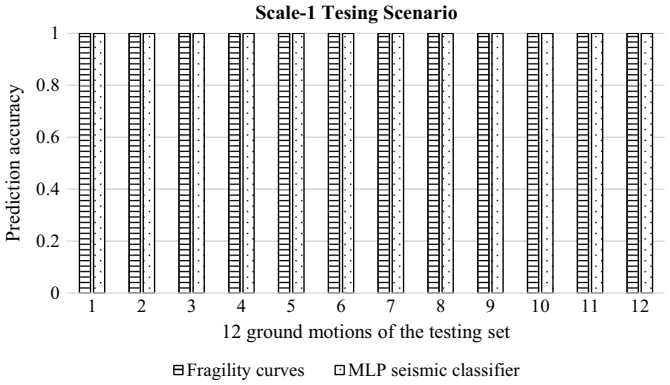

Fig. 10. Prediction accuracies of the MLP seismic classifier and traditional fragility curves under the Scale 1 testing scenario.

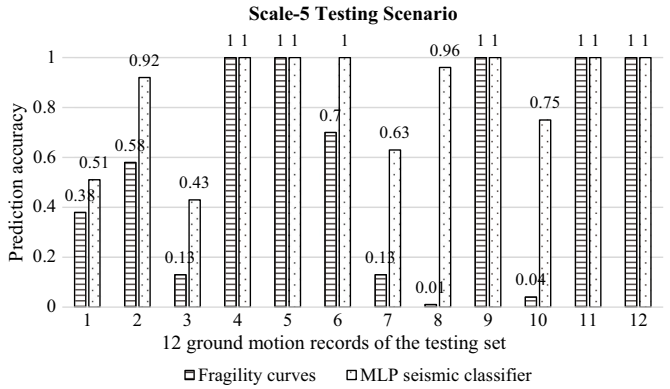

Fig. 11. Prediction accuracies of the MLP seismic classifier and traditional fragility curves under the Scale 5 testing scenario.

characteristics of near-fault (impulse) ground motions (Chen et al. 2004; Jiang et al. 2020; Zhong et al. 2020). To address the sparsity of the strong motions in the NMSZ, more validated synthesized ground motions with fully considered near-fault effects for the NMSZ (Chen et al. 2005) and historical ground motions in the WUS compatible with the magnitudes and site conditions of the CEUS can be utilized for the NLTHA and MLP training.

Due to limited structural information in the Joplin testbed data, only two structural parameters of one-story wood-frame buildings in the CEUS, i.e., the built year and the gross area, are considered. Structural properties such as stiffness, strength, and energy dissipation are hypothetically subjected to a linear deterioration relationship over time based on limited studies of wood-frame structural deterioration (Kim et al. 2006; Scotta et al. 2018). Although the hypothetical structural properties lead to reasonable natural periods of the wood-frame portfolio, more research should be conducted in the future to validate or modify the annual linearly deteriorated assumption. Moreover, although this study is focused on developing an MLP seismic classifier for one-story wood-frame residential buildings, more structural parameters should be utilized as inputs to the MLP seismic classifier for a portfolio-scale seismic damage assessment when they become available. For instance, the proposed structural parameters such as the shape of floor plan, number of stories, base-rectangular area, and openings from doors/windows and garage doors that can be obtained from a sidewalk survey should be used as structural input parameters (Lucksiri et al. 2012b). Overall, instead of grouping portfolio wood-frame residential buildings into a class and developing fragility curves by one or several representative structures, the MLP seismic classifier can incorporate more earthquake and structural uncertainties for the portfolio-scale seismic damage assessment.

Conclusions

A seismic classifier based on MLP is developed for one-story wood-frame residential buildings near the NMSZ and compared with traditional fragility curves for portfolio-scale seismic damage assessment under two testing scenarios: Scale 1 and Scale 5. In the Scale 1 testing scenario, the MLP seismic classifier and fragility curves are 100% accurate in prediction of minor damage of the building portfolio when subjected to ground motions with a spectral acceleration of less than 1 g. In the Scale 5 testing scenario, the MLP classifier and fragility curves are 85.0% and 58.1% accurate in prediction of moderate and severe damage of the building portfolio based on the average performance of 12 ground motions. Specifically, the MLP classifier and fragility curves are both 100% accurate under five testing ground motions. For the other seven testing ground motions, the MLP classifier is 13% to 95% more accurate than the fragility curves. This is mainly because the fragility curves are developed from one or several representative structures under one earthquake intensity measure, while the MLP seismic classifier can incorporate more earthquake and structural uncertainties into its input layer. Overall, the machine-learning-based seismic classifier could be a promising alternative to the fragility curves for portfolio-scale seismic damage assessment.

However, these conclusions may not be generalized in practical applications without further and broader studies for the effects of seismic regions and structural types. Site-specific ground motions, including near-fault ground motions near the NMSZ, will be employed to potentially solve the sparsity of moderate and severe damage classes when training the MLP seismic classifier. Furthermore, the MLP seismic classifier will be improved by including more structural parameters in a comprehensive wood-frame residential portfolio with different floor plans and numbers of stories.

Data Availability Statement

All raw data and materials supporting the conclusions of this article may be made available upon request from the corresponding author.

Acknowledgments

Financial support to complete this study was provided in part by the US Department of Transportation, Office of Assistant Secretary for Research and Technology under the auspices of Mid-America Transportation Center at the University of Nebraska, Lincoln (Grant No. 00059709). The authors would like to thank Dr. Chiunlin Wu for sharing his synthesized ground motions for cities near the NMSZ.

References

Atkinson, G. M., and I. A. Beresnev. 2002. "Ground motions at Memphis and St. Louis from M 7.5-8.0 earthquakes in the New Madrid Seismic Zone." *Bull. Seismol. Soc. Am.* 92 (3): 1015–1024. https://doi.org/10.1785/0120010203.

Attary, N., J. W. van de Lindt, H. Mahmoud, S. Smith, C. M. Navarro, Y. W. Kim, and J. S. Lee. 2018. "Hindcasting community-level building damage for the 2011 Joplin EF5 tornado." *Nat. Hazards* 93 (3): 1295–1316. https://doi.org/10.1007/s11069-018-3353-5.

Baker, J. W., and C. A. Cornell. 2005. "A vector-valued ground motion intensity measure consisting of spectral acceleration and epsilon." *Earthquake Eng. Struct. Dyn.* 34 (10): 1193–1217. https://doi.org/10.1002/eqe.474.

Camelo, V. S. 2003. *Dynamic characteristics of woodframe buildings*. Pasadena, CA: California Institute of Technology.

Caruana, R., and A. Niculescu-Mizil. 2006. "An empirical comparison of supervised learning algorithms." In *Proc., 23rd Int. Conf. on Machine Learning*, 161–168. New York: Association for Computer Machinery.

Cerda, P., G. Varoquaux, and B. Kégl. 2018. "Similarity encoding for learning with dirty categorical variables." *Mach. Learn.* 107 (8): 1477–1494. https://doi.org/10.1007/s10994-018-5724-2.

Chase, R. E., A. B. Liel, N. Luco, and B. W. Baird. 2019. "Seismic loss and damage in light-frame wood buildings from sequences of induced earthquakes." *Earthquake Eng. Struct. Dyn.* 48 (12): 1365–1383. https://doi.org/10.1002/eqe.3189.

Chen, G., N. Anderson, R. Luna, R. Stephenson, M. El-Engebawy, P. Silva, and R. Zoughi. 2005. *Earthquake hazards assessment and mitigation: A pilot study in the new Madrid seismic zone*. Final CIES Rep. No. 07-073. McLean, VA: Federal Highway Administration.

Chen, G., Y. Zeng, D. J. Hoffman, M. A. El-Engebawy, J. D. Rogers, and R. B. Herrmann. 2004. "Sensitivity study on near-fault rock motions within the New Madrid Seismic Zone using a composite source model." In *Proc., 11th Int. Conf. on Soil Dynamics & Earthquake Engineering and the 3rd Int. Conf. on Earthquake Geotechnical Engineering*. Rolla, MO: Missouri Univ. of Science and Technology.

Chen, S., C. Fan, and J. Pan. 2010. "Experimental study on full-scale light frame wood house under lateral load." *J. Struct. Eng.* 136 (7): 805–812. https://doi.org/10.1061/(ASCE)ST.1943-541X.0000178.

de Lautour, O. R., and P. Omenzetter. 2009. "Prediction of seismic-induced structural damage using artificial neural networks." *Eng. Struct.* 31 (2): 600–606. https://doi.org/10.1016/j.engstruct.2008.11.010.

Demuth, H., and M. Beale. 2002*Neural network toolbox—For use with MATLAB*. Natick, MA: MathWorks.

Du, A., and J. E. Padgett. 2020. "Investigation of multivariate seismic surrogate demand modeling for multi-response structural systems." *Eng. Struct.* 207 (Mar): 110210. https://doi.org/10.1016/j.engstruct.2020.110210.

Du, A., J. E. Padgett, and A. Shafieezadeh. 2020. "Influence of intensity measure selection on simulation-based regional seismic risk assessment." *Earthquake Spectra* 36 (2): 647–672. https://doi.org/10.1177/8755293019891717.

Ellingwood, B. R., D. V. Rosowsky, Y. Li, and J. H. Kim. 2004. "Fragility assessment of light-frame wood construction subjected to wind and earthquake hazards." *J. Struct. Eng.* 130 (12): 1921–1930. https://doi.org/10.1061/(ASCE)0733-9445(2004)130:12(1921).

Ellingwood, B. R., D. V. Rosowsky, and W. Pang. 2008. "Performance of light-frame wood residential construction subjected to earthquakes in regions of moderate seismicity." *J. Struct. Eng.* 134 (8): 1353–1363. https://doi.org/10.1061/(ASCE)0733-9445(2008)134:8(1353).

Fan, J., S. Upadhye, and A. Worster. 2006. "Understanding receiver operating characteristic (ROC) curves." *Can. J. Emergency Med.* 8 (1): 19–20. https://doi.org/10.1017/S1481803500013336.

FEMA. 1997. *NEHRP guidelines for the seismic rehabilitation of buildings*. FEMA-273. Washington, DC: FEMA.

Filiatrault, A., I. P. Christovasilis, A. Wanitkorkul, and J. W. van de Lindt. 2010. "Experimental seismic response of a full-scale light-frame wood building." *J. Struct. Eng.* 136 (3): 246–254. https://doi.org/10.1061/(ASCE)ST.1943-541X.0000112.

Gardoni, P., J. Van De Lindt, B. Ellingwood, T. Mcallister, J. S. Lee, H. Cutler, W. Peacock, and D. Cox. 2018. "The interdependent networked community resilience modeling environment (IN-CORE)." In *Proc., 16th European Conf. on Earthquake Engineering*, 18–21. Gaithersburg, MD: NIST.

Hafeez, G., G. Doudak, and G. McClure. 2018. "Establishing the fundamental period of light-frame wood buildings on the basis of ambient vibration tests." *Can. J. Civ. Eng.* 45 (9): 752–765. https://doi.org/10.1139/cjce-2017-0348.

Haselton, C. B., C. A. Goulet, J. Mitrani-Reiser, J. L. Beck, G. G. Deierlein, K. A. Porter, J. P. Stewart, and E. Taciroglu. 2008. *An assessment to benchmark the seismic performance of a code-conforming reinforced concrete moment-frame building*. PEER Report 2007/1. Berkeley, CA: Pacific Earthquake Engineering Research Center.

Jeong, S.-H., and A. S. Elnashai. 2007. "Probabilistic fragility analysis parameterized by fundamental response quantities." *Eng. Struct.* 29 (6): 1238–1251. https://doi.org/10.1016/j.engstruct.2006.06.026.

Jiang, L., J. Zhong, and W. Yuan. 2020. "The pulse effect on the isolation device optimization of simply supported bridges in near-fault regions." *Structures* 27 (Oct): 853–867. https://doi.org/10.1016/j.istruc.2020.06.034.

Karimzadeh, S., A. Askan, M. A. Erberik, and A. Yakut. 2018. "Seismic damage assessment based on regional synthetic ground motion dataset: A case study for Erzincan, Turkey." *Nat. Hazards* 92 (3): 1371–1397. https://doi.org/10.1007/s11069-018-3255-6.

Kasal, B., M. S. Collins, P. Paevere, and G. C. Foliente. 2004. "Design models of light frame wood buildings under lateral loads." *J. Struct. Eng.* 130 (8): 1263–1271. https://doi.org/10.1061/(ASCE)0733-9445(2004)130:8(1263).

Kim, J. H., S. M. Kent, and D. V. Rosowsky. 2006. "The effect of biological deterioration on the seismic performance of woodframe shearwalls." *Comput.-Aided Civ. Infrastruct. Eng.* 21 (3): 205–215. https://doi.org/10.1111/j.1467-8667.2006.00428.x.

Kircher, C. A., R. K. Reitherman, R. V. Whitman, and C. Arnold. 1997. "Estimation of earthquake losses to buildings." *Earthquake Spectra* 13 (4): 703–720. https://doi.org/10.1193/1.1585976.

Kostinakis, K., and K. Morfidis. 2020. "Application of artificial neural networks for the assessment of the seismic damage of buildings with irregular infills' distribution." In *Seismic behaviour and design of irregular and complex civil structures III*, 291–306. Cham, Switzerland: Springer.

Lagaros, N. D., and M. Fragiadakis. 2007. "Fragility assessment of steel frames using neural networks." *Earthquake Spectra* 23 (4): 735–752. https://doi.org/10.1193/1.2798241.

Lu, X., Y. Xu, Y. Tian, B. Cetiner, and E. Taciroglu. 2021. "A deep learning approach to rapid regional post-event seismic damage assessment using time-frequency distributions of ground motions." *Earthquake Eng. Struct. Dyn.* 50 (6): 1612–1627. https://doi.org/10.1002/eqe.3415.

Lucksiri, K., T. H. Miller, R. Gupta, S. Pei, and J. W. van de Lindt. 2012a. "Effect of plan configuration on seismic performance of single-story wood-frame dwellings." *Nat. Hazard. Rev.* 13 (1): 24–33. https://doi.org/10.1061/(ASCE)NH.1527-6996.0000061.

Lucksiri, K., T. H. Miller, R. Gupta, S. Pei, and J. W. Van De Lindt. 2012b. "A procedure for rapid visual screening for seismic safety of wood-frame dwellings with plan irregularity." *Eng. Struct.* 36 (Mar): 351–359. https://doi.org/10.1016/j.engstruct.2011.12.023.

Luco, N., and P. Bazzurro. 2007. "Does amplitude scaling of ground motion records result in biased nonlinear structural drift responses?" *Earthquake Eng. Struct. Dyn.* 36 (13): 1813–1835. https://doi.org/10.1002/eqe.695.

Luco, N., and C. A. Cornell. 2007. "Structure-specific scalar intensity measures for near-source and ordinary earthquake ground motions." *Earthquake Spectra* 23 (2): 357–392. https://doi.org/10.1193/1.2723158.

Mangalathu, S., G. Heo, and J. S. Jeon. 2018. "Artificial neural network based multi-dimensional fragility development of skewed concrete bridge classes." *Eng. Struct.* 162 (May): 166–176. https://doi.org/10.1016/j.engstruct.2018.01.053.

Memari, M., N. Attary, H. Masoomi, H. Mahmoud, J. W. van de Lindt, S. F. Pilkington, and M. R. Ameri. 2018. "Minimal building fragility portfolio for damage assessment of communities subjected to tornadoes." *J. Struct. Eng.* 144 (7): 04018072. https://doi.org/10.1061/(ASCE)ST.1943-541X.0002047.

Morfidis, K., and K. Kostinakis. 2018. "Approaches to the rapid seismic damage prediction of r/c buildings using artificial neural networks." *Eng. Struct.* 165 (Jun): 120–141. https://doi.org/10.1016/j.engstruct.2018.03.028.

Morfidis, K., and K. Kostinakis. 2019. "Comparative evaluation of MFP and RBF neural networks' ability for instant estimation of r/c buildings' seismic damage level." *Eng. Struct.* 197 (Oct): 109436. https://doi.org/10.1016/j.engstruct.2019.109436.

Pang, W., D. V. Rosowsky, B. R. Ellingwood, and Y. Wang. 2009. "Seismic fragility analysis and retrofit of conventional residential wood-frame structures in the Central United States." *J. Struct. Eng.* 135 (3): 262–271. https://doi.org/10.1061/(ASCE)0733-9445(2009)135:3(262).

Pei, S., J. W. van de Lindt, N. Wehbe, and H. Liu. 2013. "Experimental study of collapse limits for wood frame shear walls." *J. Struct. Eng.* 139 (9): 1489–1497. https://doi.org/10.1061/(ASCE)ST.1943-541X.0000730.

Ren, Y., P. Zhao, Y. Sheng, D. Yao, and Z. Xu. 2017. "Robust softmax regression for multi-class classification with self-paced learning." In *Proc., IJCAI Int. Joint Conf. on Artificial Intelligence*, 2641–2647. Washington, DC: AAAI Press.

Scotta, R., D. Trutalli, L. Marchi, and L. Pozza. 2018. "On the anchoring of timber walls to foundations: Available strategies to prevent wood deterioration and on-site installation problems." *Procedia Struct. Integrity* 11 (Jan): 282–289. https://doi.org/10.1016/j.prostr.2018.11.037.

Singh, D., and B. Singh. 2020. "Investigating the impact of data normalization on classification performance." *Appl. Soft Comput.* 97 (Dec): 105524. https://doi.org/10.1016/j.asoc.2019.105524.

Soltis, L. A., and R. H. Falk. 1992. "Seismic performance of low-rise wood buildings." *Shock Vibr. Dig.* 24 (12): 3–6. https://doi.org/10.1177/058310249202401202.

van de Lindt, J. W. 2005. "Damage-based seismic reliability concept for woodframe structures." *J. Struct. Eng.* 131 (4): 668–675. https://doi.org/10.1061/(ASCE)0733-9445(2005)131:4(668).

van de Lindt, J. W., S. Pei, S. E. Pryor, H. Shimizu, and H. Isoda. 2010. "Experimental seismic response of a full-scale six-story light-frame wood building." *J. Struct. Eng.* 136 (10): 1262–1272. https://doi.org/10.1061/(ASCE)ST.1943-541X.0000222.

Vaseghiamiri, S., M. Mahsuli, M. A. Ghannad, and F. Zareian. 2020. "Surrogate SDOF models for probabilistic performance assessment of multistory buildings: Methodology and application for steel special moment frames." *Eng. Struct.* 212 (Jun): 110276. https://doi.org/10.1016/j.engstruct.2020.110276.

Wald, D. J., B. C. Worden, V. Quitoriano, and K. L. Pankow. 2006. *ShakeMap manual: Technical manual, user's guide, and software guide*. Reston, VA: USGS.

Wang, Z., N. Pedroni, I. Zentner, and E. Zio. 2018. "Seismic fragility analysis with artificial neural networks: Application to nuclear power plant equipment." *Eng. Struct.* 162 (May): 213–225. https://doi.org/10.1016/j.engstruct.2018.02.024.

Wen, Y. K., M. Eeri, C. L. Wu, and M. Eeri. 2001. "Uniform hazard ground motions for mid-America cities." *Earthquake Spectra* 17 (2): 359–384. https://doi.org/10.1193/1.1586179.

Xu, Y., X. Lu, Y. Tian, and Y. Huang. 2020. "Real-time seismic damage prediction and comparison of various ground motion intensity measures based on machine learning." *J. Earthquake Eng.* 26 (8): 4259–4279. https://doi.org/10.1080/13632469.2020.1826371.

Yang, T., X. Yuan, J. Zhong, and W. Yuan. 2023. "Near-fault pulse seismic ductility spectra for bridge columns based on machine learning." *Soil Dyn. Earthquake Eng.* 164 (Jan): 107582. https://doi.org/10.1016/j.soildyn.2022.107582.

Yi, Z. 2020. *Performance-based analytics-driven seismic retrofit of woodframe buildings*. Los Angeles: Univ. of California.

Yi, Z., and H. Burton. 2020. "Machine learning based regional seismic retrofit design optimization of soft-story woodframe buildings." In *Proc., 17th World Conf. on Earthquake Engineering*. Kanpur, India: National Information Centre for Earthquake Engineering.

Yuan, X., G. Chen, P. Jiao, L. Li, J. Han, and H. Zhang. 2022. "A neural network-based multivariate seismic classifier for simultaneous post-earthquake fragility estimation and damage classification." *Eng. Struct.* 255 (Mar): 113918. https://doi.org/10.1016/j.engstruct.2022.113918.

Yuan, X., D. Tanksley, P. Jiao, L. Li, G. Chen, and D. Wunsch. 2021. "Encoding rime-series ground motions as images for convolutional neural networks-based seismic damage evaluation." *Front. Built Environ.* 7 (Apr): 660103. https://doi.org/10.3389/fbuil.2021.660103.

Zhao, Y., H. Hu, L. Bai, M. Tang, H. Chen, and D. Su. 2021. "Fragility analyses of bridge structures using the logarithmic piecewise function-based probabilistic seismic demand model." *Sustainability* 13 (14): 7814. https://doi.org/10.3390/su13147814.

Zhong, J., L. Jiang, Y. Pang, and W. Yuan. 2020. "Near-fault seismic risk assessment of simply supported bridges." *Earthquake Spectra* 36 (4): 1645–1669. https://doi.org/10.1177/8755293020935145.